First-principles study of As, Sb, and Bi electronic properties

X. Gonze and J.-P. Michenaud
Laboratoire de Physico-Chimie et de Physique des Matériaux, Université Catholique de Louvain, B-1348 Louvain-la-Neuve, Belgium

J.-P. Vigneron
Institute for Studies in Interface Sciences (ISIS), Facultés Universitaires Notre-Dame de la Paix, 61 rue de Bruxelles, B-5000 Namur, Belgium

(Received 2 November 1989; revised manuscript received 16 March 1990)

Arsenic, antimony, and bismuth, three group-V elements which crystallize in the rhomboedral $A7$ structure, are well-known semimetals. Going from As to Sb to Bi, the unit-cell parameters increase, as well as the strength of the spin-orbit interaction, leading to quantitative differences in the electronic properties of these materials. By means of the standard Hohenberg-Kohn-Sham density-functional approach using the Ceperley-Alder exchange-correlation energy as parametrized by Perdew and Zunger, we have carefully compared the following properties of each semimetal: band structure, electronic density of charge, density of states, and Fermi surface. The role of spin-orbit coupling, which is noticeable in Bi, has been emphasized. The numerical accuracy of the calculation has been strictly controlled, in order to provide reliable comparison between theoretical results and experimental data for the density of states, number of free carriers, and Fermi surface. The good agreement obtained for Fermi surfaces is somewhat unexpected.

I. INTRODUCTION

Crystalline As, Sb, and Bi share two related peculiar features: a slight departure from an exact cubic crystallographic structure, and a weak overlap between valence and conduction bands that leads to a small built-in density of free electrons and holes.[1] This latter peculiarity, namely, the semimetallic state, leads to an enhancement of many transport coefficients. As a striking example, bismuth allowed the discoveries of the Seebeck effect and other related thermomagnetic effects. Owing to the smallness of the effective masses, oscillatory phenomena in a magnetic field, such as de Haas–van Alphen and Shubnikov–de Haas effects, were also observed for the first time in Bi.[1]

Since the early 1960s, a variety of independent measurements have established the main features of the band structure and the shape of the Fermi surface.[2] From the theoretical point of view, many band-structure and total-energy investigations have been carried out. We can mention an early tight-binding calculation for Bi,[3] the qualitative analysis of bonding in group-V rhomboedral compounds,[4] and different semiempirical or approximate studies of As,[5–9] Sb,[10,11] and Bi.[11,12] The investigation of these materials by precise *ab initio* techniques has only been undertaken[13–16] recently, and has concentrated mainly on the structural properties.

We have performed state-of-the-art *ab initio* calculations of the following As, Sb, and Bi electronic properties: valence charge density, band structure, charge density for each band, density of states (DOS), and Fermi surface. The precision requirement was particularly stringent for this latter property. Nevertheless, we have been able to satisfactorily reproduce the experimental Fermi surface shapes and number of free carriers, which are very sensitive quantities. The role of spin-orbit (s.o.) coupling, which is noticeable in Bi, has been emphasized.

The paper starts with a presentation of the atomic electronic structure of the three elements, and with the description of their respective crystalline states (Sec. II). Then, we critically discuss the *ab initio* theoretical method we used to study the above-mentioned properties (Sec. III): a self-consistent density-functional approach, using *ab initio* nonlocal pseudopotentials and a local-density approximation for exchange and correlation. Numerical results as well as a comparison with experimental results [Fermi surface, x-ray photoelectron spectroscopy (XPS) spectra] are presented in Sec. IV. Finally, we discuss the unexpected good agreement between theory and experiment.

II. ATOMIC PROPERTIES AND $A7$ STRUCTURE

The knowledge of the atomic electronic properties of As, Sb, and Bi shed light on the electronic properties of their corresponding crystalline state.

The external electron configuration of As, Sb, and Bi is s^2p^3, plus a complete d shell. Those s and p levels will mix in the solid, while the other d-electron and core-electron levels will remain practically unchanged. This means that only the five s and p electrons will be considered as valence electrons, while the others will be considered as being part of the ionic core.

The s levels lie about 9 eV lower than the p levels.[17] These p levels further split into two levels due to s.o. effects. The amplitude of the p-level splitting increases with the element atomic number: approximately 0.3 eV for As, 0.6 eV for Sb, and 1.5 eV for Bi.[5,17] These values

provide a measure of the spin-orbit coupling effects in solids. In the case of As and Sb, this coupling leads to the suppression of several specific degeneracies, which can be observed in the band structure, with little incidence on the global electronic properties. In the case of Bi, however, the effect turns out to be highly significant. In this paper we shall actually be examining four different materials: the *ab initio* As, Sb, and Bi, and also the fictitious "Bi without spin-orbit coupling" for which we consider the pseudopotential without its **L·S** part.

The minimum energy structure for these three elements corresponds to the rhomboedral $A7$ structure [Fig. 1(a)]. This rhomboedral unit cell contains two atoms. It is based on the three vectors starting from the atom labeled O'. The atom labeled A is very close to the center of the cell, but slightly displaced along the trigonal axis of the rhomboedral cell. Centers of inversion are present along the trigonal axis, at the middle of the OA and $O'A$ segments, and at the center of the segments connecting two nearest-neighbor atoms and two next-nearest-neighbor atoms.

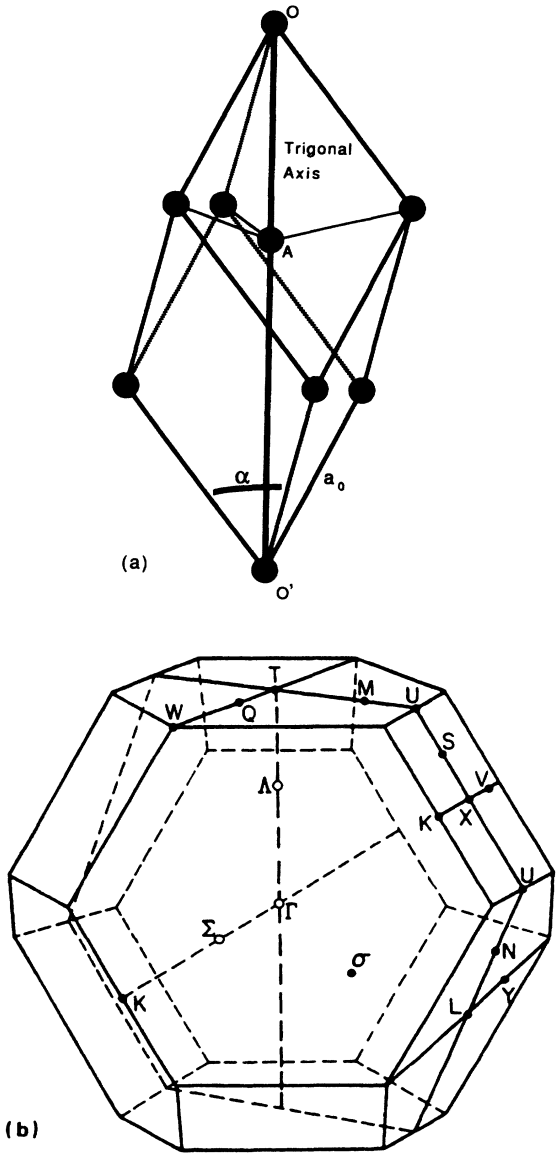

FIG. 1. (a) $A7$ rhomboedral unit cell. As, Sb, and Bi all crystallize in this structure. The A atom is close to the center of the cell, but slightly displaced along the trigonal axis OO'. (b) The corresponding Brillouin zone.

TABLE I. Crystallographic parameters for the unit cell of As, Sb, and Bi.

	As	Sb	Bi
a_0 (Å)	4.1018	4.4898	4.7236
α (deg)	54.554	57.233	57.35
z	0.455 28	0.467 24	0.468 14
a_{NN}	2.5165	2.9023	3.0624

Three parameters completely determine the unit cell and atom positions: the length a_0 of the rhomboedral-cell vectors, the rhomboedral angle α, and the position of the second atom along the trigonal axis, determined by the ratio $z = OA/OO'$. Table I gives these quantities for the three semimetals,[18] and also the nearest-neighbor (NN) distance a_{NN} (or bond length), which increases by about 15% from As to Sb, and by about 5% from Sb to Bi. More details on the $A7$ structure can be found in Needs *et al.*[13] These lattice constants and atomic positions will be used in Sec. III. Figure 1(b) represents the Brillouin zone; the usual notation for symmetry points has been used.[19]

III. THEORETICAL METHOD

We performed a quite standard Hohenberg-Kohn-Sham density-functional calculation[20] with the Ceperley-Alder exchange-correlation energy as parametrized by Perdew and Zunger.[21] The ionic core potentials were replaced by *ab initio* ionic pseudopotentials, of the norm-conserving type, as given by the complete table of Bachelet *et al.*[22]

Figure 2 presents the four ionic pseudopotentials, where each angular part is labeled using the usual atomic notation, and the dotted curve represents the "bare" Coulombic potential $-Z/r$ (atomic units), this one being the asymptotic limit of all pseudopotential components. The increasing influence of spin-orbit coupling is clearly seen in its effects on the p and d levels. We used a plane-wave basis set (up to 620 plane waves, depending on the required accuracy) within the framework of the momentum-space formalism,[23] and solved the self-consistent Schrödinger equation using the algorithm of Wood and Zunger,[24] and a modified "simple-mixing" scheme[25] for the density self-consistency.

In connection with this treatment of semimetal electronic structure, three technical points are worth mentioning: treatment of spin-orbit coupling, treatment of the band occupation, and Brillouin-zone sampling procedure. Besides a complete description of the method used, an extensive study of the uncertainties associated with each numerical parameter or approximation is required (see the Appendix for details). In view of the

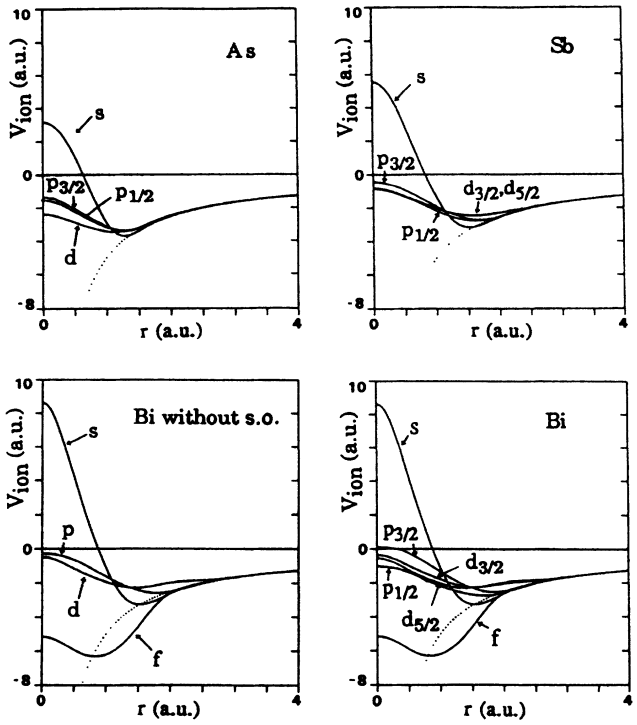

FIG. 2. *Ab initio* nonlocal relativistic atomic pseudopotentials for As,Sb,Bi without s.o. coupling, and Bi, as calculated by Bachelet, Hamann, and Schlüter (Ref. 19) (atomic Hartree units). The dotted curves correspond to the Coulombic potential of a pointlike $Z=5$ charge.

small (500–200 meV for As and Sb) or even very small (30–50 meV for Bi) overlaps, the maximum truncation error on energies at the Fermi level has been reduced to 20 meV for As and Sb, and 5 meV for Bi. At other points in the Brillouin zone, for the first eight bands, the accuracy requirement is somewhat less stringent. In the Appendix, we summarize the estimated uncertainties obtained for each semimetal.

In the pseudopotential method, spin-orbit coupling arises naturally in the $\mathbf{L}\cdot\mathbf{S}$ form.[22] The general expression for the matrix element of the spin-orbit pseudopotential between two plane waves can be found in Refs. 26 and 27. The diagonalization can be performed following two different schemes: both have been used in the present study. In the first method,[28] which is exact but also very demanding from a computational point of view, the entire matrix including up and down spin, is considered, and solved using an iterative method.[24] In the second method (restricted space method),[16] the first eight eigenvectors of the Hamiltonian without spin orbit are calculated, and the complete Hamiltonian is then solved in a subspace spanned by these eight eigenvectors (doubled to accommodate the spin degree of freedom). The analysis described in the Appendix shows that the restricted-space treatment can safely be used for As and Sb, while a full treatment of spin-orbit coupling is needed for Bi.

The number of conduction electrons or valence holes is found experimentally to be very small for bismuth ($<2\times10^{-5}$ per unit cell) and small, yet 2 orders of magnitude larger, for antimony and arsenic ($<3\times10^{-3}$ and $<10^{-2}$, respectively).[1] The numerical results turn out to be of the same order of magnitude. We can thus construct the charge density considering the material as a semiconductor, with the first five bands completely filled. This treatment of semimetals, described in a previous paper,[16] is substantiated by data given in the Appendix.

The number of special points[29] needed to sample the Brillouin zone is also of interest. Using symmetry, we can limit the investigated zone to $\frac{1}{12}$ of the entire Brillouin zone. The use of 60 special points to obtain the self-consistent density has been the general rule in this investigation, where the accuracy on eigenvalues (near Fermi energy) is of utmost importance. The investigation of Fermi surfaces has been conducted using about 200 **k** points for each hole or electron pocket in Sb and As, and 50 **k** points in Bi. For the density of states (DOS) we have used the Lehmann-Taut analytical tetrahedron method[30] with 95 points in the irreducible part of the Brillouin zone.

The problems inherent to the use of the density-functional formalism will be discussed more specifically in the final part of this paper.

IV. RESULTS

A. The total charge density

Figure 3 and 4 show, for each element , the total pseudocharge density, in two different planes: the first plane $(1\bar{1}0)$—a mirror plane—contains the trigonal axis; the second plane (111) is perpendicular to the trigonal axis and thus shows up the trigonal symmetry. The use of a pseudopotential does not alter the density in the region of interest: the "cutoff radius"[31] is in our case always smaller than the radius where the density is maximum. Mattheis *et al.*[15] had already proposed a similar graph for Arsenic, in the mirror plane. Their results, using the linear augmented-plane-wave method, are similar to ours (see also Ref. 8).

In the mirror plane, the isodensity lines clearly show the main features of the binding. This binding is similar for all semimetals studied here: in the plane containing the trigonal axis, each atom has one bond, and is also connected to two other atoms outside this plane, due to the trigonal symmetry. We can therefore imagine the material as an assembly of pairs of parallel planes stacked along the trigonal axis. This stacking of pairs of planes can explain the relatively easy cleaving property of this type of monocrystals. The anisotropy of these crystals is, however, less obvious than for other two-dimensional materials, such as graphite.

The extinction of spin-orbit coupling for bismuth introduces a very slight modification of the charge density, too small to be represented on contour charts similar to Fig. 3.

B. The band structure

Figure 5 compares the band structure of the three elements, and also that of bismuth calculated *without* taking

into account the spin-orbit coupling. One can clearly distinguish the two s bands, below the six p bands, three of the latter being occupied. Although the band structures are very similar, some interesting differences should be emphasized.

First, the total width of the first two bands at the Γ point decreases from As to Sb to Bi. This is related to the aforementioned increase of the nearest-neighbor distance, which reduces the overlap between atomic s levels.

These two bands are practically unaffected by the

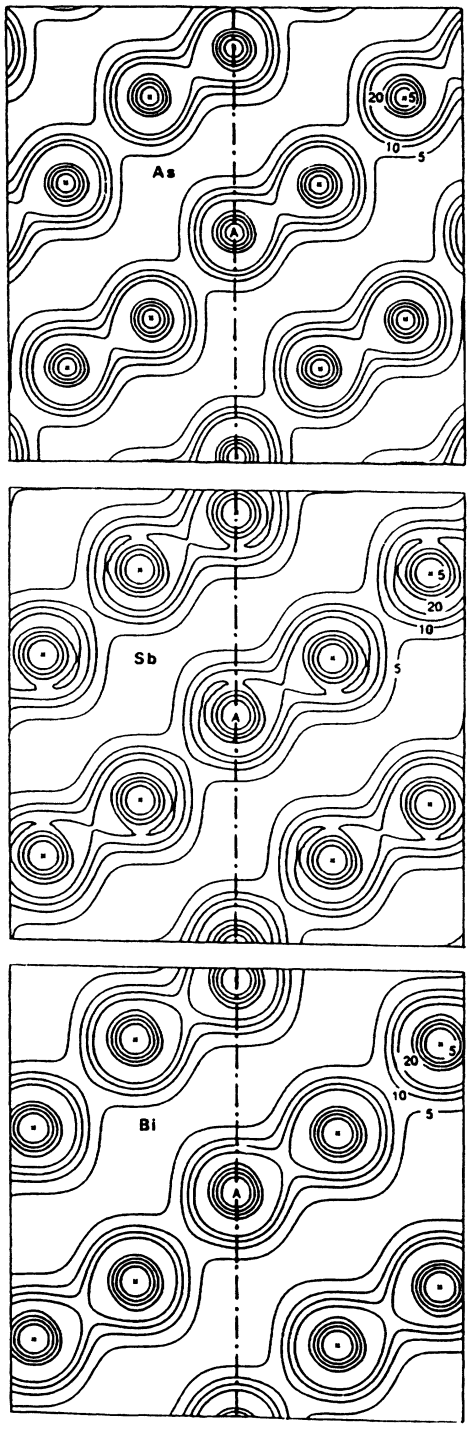

FIG. 3. Valence electron pseudocharge densities in the $(1\bar{1}0)$ plane for As, Sb, and Bi. The contour interval is in units of 5.0 electrons per primitive cell. The dot-dashed line represents the trigonal axis. Crosses indicate atoms. The atoms marked A correspond to the atoms marked A in Fig. 4.

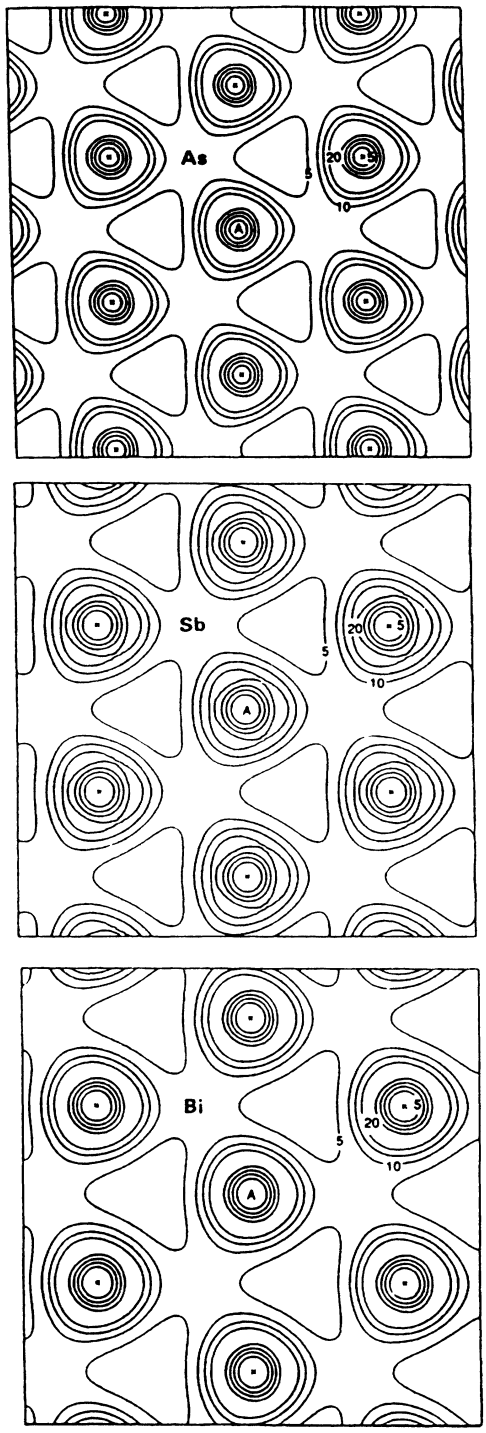

FIG. 4. Valence electron pseudocharge densities in the (111) plane for As, Sb, and Bi. The contour interval is in units of 5.0 electrons per primitive cell. This (111) plane shows up the trigonal symmetry. Crosses indicate atoms positions. The atoms marked A correspond to the atoms marked A in Fig. 3.

spin-orbit coupling, even for bismuth. This is not surprising since the spin-orbit coupling is of the $\mathbf{L}\cdot\mathbf{S}$ form, and these bands originate mainly from the atomic s level, with $L=0$. The increasing effect of spin-orbit coupling is clearly visible on the $\Gamma-T$ and $\Gamma-X$ lines, for the p-level bands. The degeneracy along the $\Gamma-T$ line (see bismuth without spin-orbit coupling) is slightly relaxed in As and Sb, while in Bi (with s.o.), the spin-orbit coupling is so strong that the comparison is difficult. The magnitude of this effect can be predicted from the atomic splitting we have mentioned in the first paragraph (i.e., 0.36 eV for As, 0.6 eV for Sb, 1.5 eV for Bi).

The small overlap between conduction and valence bands and the Fermi surface will be discussed in Sec. IV E.

C. Partial charge densities

The unit cell contains two atoms. The atomic s level generates two distinct bands, each being degenerate with respect to the spin: they can be called "bonding" and "antibonding" by analogy with the usual nomenclature of the theory of homonuclear diatomic molecules.[4,32]

For As (Fig. 6), Sb (Fig. 7), and Bi (Fig. 8), we have represented the band-by-band charge densities of the first band (bonding s level), of the second band (antibonding s level) and of the third, fourth, and fifth bands (occupied p levels), in the mirror plane. It appears that the charge densities of s bands are more centered on the atoms than those of p bands. While the densities of the first two bands are very similar for the three elements, with marked bonding and antibonding types, the maximum of the density of the p bands, in this plane, changes from mainly antibonding localization for As, to mainly bonding localization for Bi. Nevertheless, even for As, the total number of electrons contributing to the p-level bonding is greater than those contributing to antibonding.

As for the total charge density, the spin-orbit coupling has only a small effect, which cannot be represented in these figures.

D. DOS and XPS spectra

Figure 9(a) presents the calculated DOS for the valence states. Figures 9(b) and 9(c) compare the 0.6-eV Gaussian convolution of this DOS with the experimental XPS results obtained by Ley *et al.*[33] (who estimated the experimental broadening at 0.55 eV).

The contributions of s and p bands are clearly marked. The locations of the peaks are well reproduced, in partic-

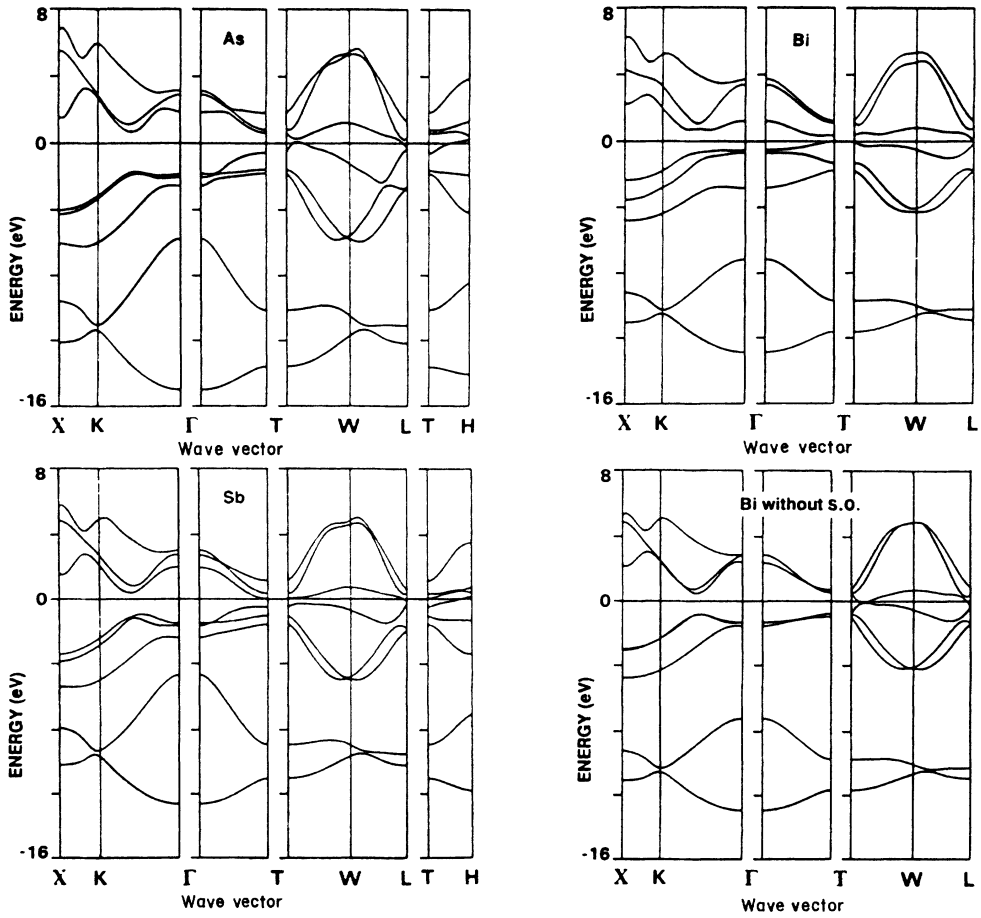

FIG. 5. Band structure for As, Sb, Bi, and Bi without s.o. coupling, along different lines in the Brillouin zone.

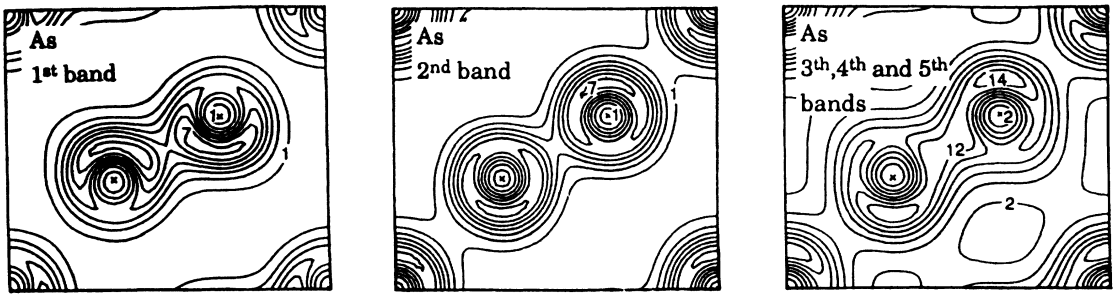

FIG. 6. Band-by-band pseudocharge densities in the $(1\bar{1}0)$ plane for As. The leftmost and center graphs give the contribution of the bonding s band and the antibonding s band, with a contour interval in units of 1.0 electrons per primitive cell, while the rightmost graph gives the contribution of the three occupied p bands, with the contour interval in units of 2.0 electrons per primitive cell.

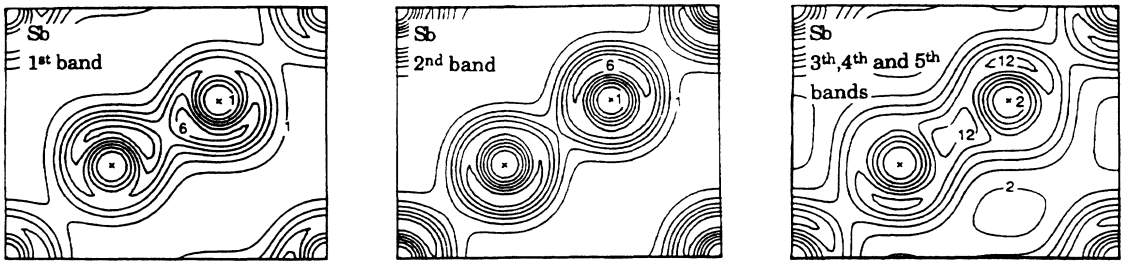

FIG. 7. Band-by-band pseudocharge densities in the $(1\bar{1}0)$ plane for Sb. The leftmost and center graphs give the contribution of the bonding s band and the antibonding s band, with a contour interval in units of 1.0 electrons per primitive cell, while the rightmost graph gives the contribution of the three occupied p bands, with the contour interval in units of 2.0 electrons per primitive cell.

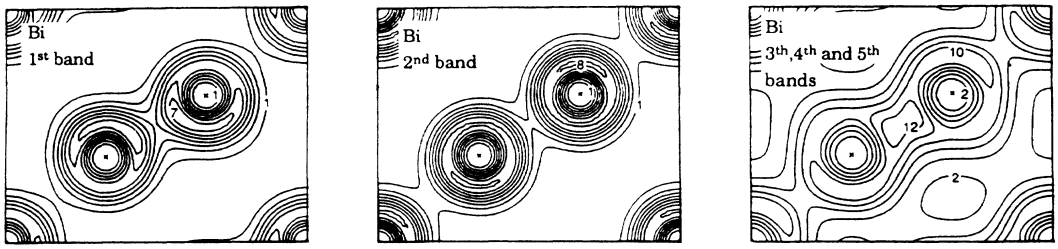

FIG. 8. Band-by-band pseudocharge densities in the $(1\bar{1}0)$ plane for Bi. The leftmost and center graphs give the contribution of the bonding s band and the antibonding s band, with a contour interval in units of 1.0 electrons per primitive cell, while the rightmost graph gives the contribution of the three occupied p bands, with the contour interval in units of 2.0 electrons per primitive cell.

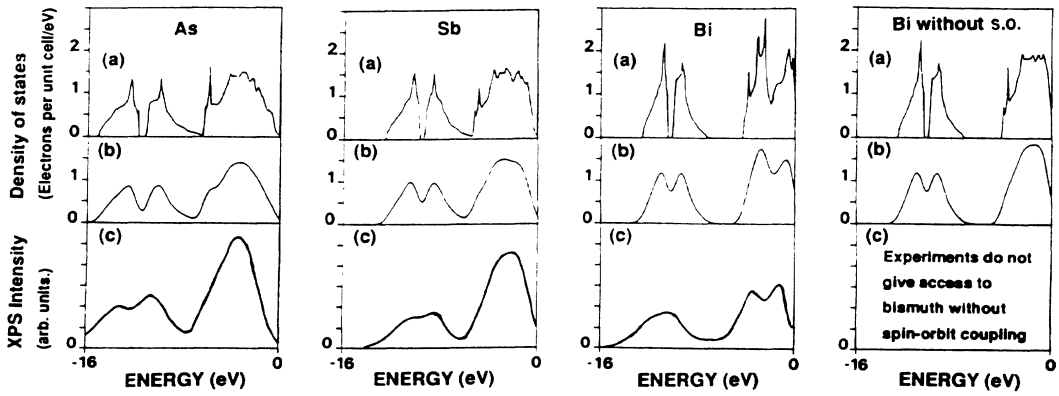

FIG. 9. For the four "elements" As, Sb, Bi, and Bi without s.o. coupling, comparison of (a) theoretical (DOS), (b) theoretical smoothed DOS (0.6 eV Gaussian smoothing), and (c) experimental XPS from Ref. 29. The experimental XPS spectra for Bi without spin-orbit coupling is, of course, missing.

ular, the *splitting of the major peak in bismuth* which disappears in the fictitious Bi without spin-orbit coupling. Arsenic[15] and antimony do not present such a splitting. This splitting, which is a peculiar feature of the Bi density of states (absent from As and Sb spectra) is, therefore, one of the direct consequences of the relativistic behavior of electrons.

While the qualitative features seem quite relevant, the precise values of the computed amplitudes are less satisfactory, because the matrix elements between initial and final states, required to reproduce the experimental XPS spectra, have been neglected. In any case, the energy of the characteristic peaks has a very weak dependence on the matrix elements. This allows to match experimental and theoretical results.

E. Semimetallic behavior, number of carriers, and Fermi surface

A variety of experimental and semiempirical theoretical investigations have already established the main features of the band scheme near the Fermi level. In the three materials, an overlap between the fifth and sixth bands creates free electrons at point L, and free holes at point H (for As and Sb) or point T (for Bi).[1-16] This overlap decreases from As to Sb to Bi. In bismuth, the electron and hole pockets are nearly perfect ellipsoids. In Sb and As, the electron pockets depart a little from ellipsoids, while the hole pockets are much more tortuous.

On Fig. 5, the slight overlap between valence and conduction bands is hardly visible for Bismuth (T and L points), and somewhat more apparent for Sb and As (H and L points). The magnitude and the location of these overlaps are in good agreement with experimental results.

Table II summarizes the overlap values, the coordinates of the maximum of the valence band and the carrier densities. The free hole and electron pockets are located in the Brillouin zone at places commonly accepted by other authors. (Note that our result comes from first principles; the only experimental inputs are the lattice parameters.) The spin-orbit coupling is very important in bismuth since, without it, the holes would not be obtained in the experimentally observed location point T.[16]

The parameters of the bismuth electron and hole pockets, as well as antimony and arsenic electron pockets, are presented in Table III. We also present the hole Fermi surface for Sb and As, Fig. 10. The form of this Fermi surface is, in fact, quite similar to that computed by Lin and Falicov,[7] or Rose and Schuchardt.[11]

Interesting features of the arsenic hole Fermi surface

TABLE II. Characteristics of the semimetallic state. (a) Difference between the Fermi energy and the extremal energy for electrons (eV). (b) Difference between the Fermi energy and the extremal energy for holes (eV). (c) Coordinates of the H point, for As and Sb, expressed in trigonal coordinates [P. J. Lin and L. M. Falicov, Phys. Rev. **142**, 441 (1966)]. (d) Carrier density (electrons/unit cell).

	As	Sb	Bi
		(a)	
Electrons			
Present work	0.408[a]	0.206[a]	0.0183[a]
Other theoretical	0.367[d]	0.115,[e] 0.108[g]	0.016,[e] 0.027[g]
Experimental	0.202,[b] 0.190[h]	0.093–0.160[b,e]	0.02–0.030[b,c,e]
		(b)	
Holes			
Present work	0.202[a]	0.114[a]	0.0234[a]
Other theoretical	0.362[d]	0.119,[e] 0.142[g]	0.008,[e] 0.012[g]
Experimental	0.154,[b] 0.177[h]	0.0844[b]	0.006–0.016[b,c,e]
		(c)	
Present work	(0.37,0.194,0.194)[a]	(0.350,0.163,0.163)[a]	
Other theoretical	(0.376,0.204,0.204)[d]	(0.372,0.101,0.101)[e] and (0.393,0.245,0.245)[f]	
		(d)	
Present work	0.0134[a]	0.004 51[a]	4.0×10^{-5}[a]
Experimental	0.0085,[b] 0.0092[h]	0.002 24[b]	1.9×10^{-5},[b] 2.1×10^{-5}[c]

[a]Present work.
[b]J.-P. Issi, Aust. J. Phys. **32**, 585 (1979), and references therein.
[c]V. S. Edel'man, Adv. Phys. **25**, 555 (1976); Usp. Fiz. Nauk **123**, 257 (1977) [Sov. Phys.—Usp. **20**, 819 (1977)].
[d]P. J. Lin and L. M. Falicov, Phys. Rev. **142**, 441 (1966).
[e] J. Rose and R. Schuchardt, Phys. Status Solidi B **117**, 213 (1983), and references therein.
[f]L. M. Falicov and P. J. Lin, Phys. Rev. **141**, 562 (1966).
[g]S. Golin, Phys. Rev. **166**, 643 (1968).
[h]M. G. Priestley, L. R. Windmiller, J. B. Ketterson, and Y. Eckstein, Phys. Rev. **154**, 671 (1967).

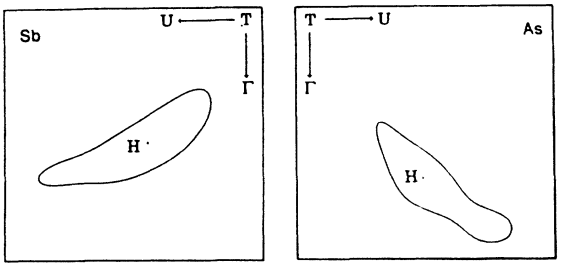

FIG. 10. Hole Fermi surfaces in the $(1\bar{1}0)$ mirror plane, for Sb and As. The size of the graph is 0.3184 a.u. for As and 0.2319 a.u. for Sb. Coordinates of the H point are given in Table II(c). The T point is at the upper left corner in the As graph, but is outside the Sb graph. Arrows only indicate directions parallel to the related symmetry axes.

are the "necks" which connect the pockets, generating the Lin and Falicov "monster."[7] Experimental results[34] and semiempirical calculations[7] show that the very thin necks form an angle of 9.6°–11° with the trigonal direction; the maximum energy when they cross the *TWU* plane is 10.6 meV above the Fermi energy and the coordinates of the latter point are (0.4616,0.5,0.5383). We found, respectively, 6.2°, 3.3 meV under the Fermi level, and (0.449,0.5,0.551). If we recall that the accuracy is of the order of 10 meV, the agreement is excellent.

The complete set of values, when compared to experimental values, is as good as other theoretical (semiempirical) calculations. It seems that the only systematic deviation from experiment is a larger number of carriers. It can be related to either a too large overlap, or a too large effective mass. In the present study, both can be present, alone or together. Distortions in the shapes of the pockets are nonsystematic.

TABLE III. Fermi surface parameters: principal momenta of the (quasi)ellipsoids for electron pockets of the three semimetals, and for the hole pocket of Bi. Axis 2 is the binary axis, axis 3 is the trigonal axis, and axis 1 is perpendicular to the other two axes. Axis 1′ is, in the mirror plane, the direction of largest k value, and axis 3′ is, in the mirror plane, the direction of least k value (1′ and 3′ are not orthogonal in general, but a large difference arises only in the case of arsenic). The φ angles are the angles between primed axes and nonprimed axes, with the sign defined in the corresponding experimental paper. All values are in atomic units.

		Present calculation	Experiment
As electrons	$k_{1'}$	0.207	0.171[a]
	k_2	0.050	0.047[a]
	$k_{3'}$	0.038	0.038[a]
	φ_1	12.0°	9.0°[a]
	φ_3	0.4°	3.6°[a]
Sb electrons	$k_{1'}$	0.134	0.157[b]
	k_2	0.028	0.022[b]
	$k_{3'}$	0.028	0.022[b]
	φ	4°	7°[b]
Bi electrons	$k_{1'}$	0.0392	0.0395[c]
	k_2	0.0043	0.0028[c]
	$k_{3'}$	0.0050	0.0037[c]
	φ	12°50′	6°23′[c]
Bi holes	k_1	0.0100	0.0073[c]
	k_2	0.0100	0.0073[c]
	k_3	0.0243	0.0244[c]

[a]M. G. Priestley, L. R. Windmiller, J. B. Ketterson, and Y. Eckstein, Phys. Rev. **154**, 671 (1967), from the extremal areas, with an ellipsoidal approximation.

[b]I. R. H. Herrod, C. A. Gage, and R. G. Goodrich, Phys. Rev. **134**, B1033 (1971); A. P. Korolyuk and L. Ya. Matsakov, Zh. Eksp. Teor. Fiz. **13**, 1860 (1971).

[c]V. S. Edel'man, Adv. Phys. **25**, 555 (1976); V. S. Edel'man, Usp. Fiz. Nauk **123**, 257 (1977) [Sov. Phys.—Usp. **20**, 819 (1977)].

V. DISCUSSION AND CONCLUSION

The present study is *ab initio*, except for the crystallographic parameters. Our method has been submitted to a particularly stringent test, in particular, for the Fermi surface calculation. The numerical uncertainties have been identified and, when possible, systematically reduced. In this respect, our numerical treatment of the semimetallic behavior has been shown to be adequate: As, Sb, and Bi can be treated as semiconductors for the generation of the charge density.

The electronic properties of the three semimetals have been related to the electronic properties of the atoms, leading to a qualitative comprehension of the bonding of the crystalline solid. This bonding can be decomposed into contributions of each particular band, using the partial density of charge; this provides an obvious characterization of bands as bonding and antibonding s-level and p-level bands. The band structures of the three elements, as well as bismuth considered without spin-orbit coupling, have been analyzed and compared. The DOS have also been investigated, and a comparison of DOS and XPS spectra have revealed similar features: in particular, an interesting peak splitting in bismuth, as a consequence of the spin-orbit coupling. This spin-orbit coupling, while relatively unimportant for the charge-density calculation, is not negligible for the eigenvalue band structure, and the related properties, i.e., DOS and Fermi surface. In bismuth, its influence is noticeable, not only qualitatively, but also quantitatively.

We have generated the Fermi surfaces of the three elements, with a good qualitative result, and, as only systematic deviation, a somewhat larger number of carriers. This fact raises some interesting questions. Within the framework of the density-functional theory, the total energy and charge density are calculated rigorously, whereas the direct identification of Kohn-Sham eigenenergies with the real band structure has little theoretical foundation. Indeed, it is well known that this approach fails to give correct values of the band gaps for semiconductors and insulators. The discrepancy between theoretical and experimental gaps is frequently of the order 0.5–1.0 eV (Ref. 35) sometimes larger.

Quite recently, with the use of the *GW* method of Hedin[35] (including self-energy corrections), theoretical values of the gap have been shown to agree with experi-

mental ones (to the precision of 0.1–0.2 eV). The *GW* studies were not restricted to a band-gap calculation, but aimed at calculating the band structure at other points in the Brillouin zone and achieved this goal with similar success.

In the present work, without self-energy corrections, we have addressed other interesting features: the shape of the Fermi surface, and the number of free carriers. From the above-mentioned failures of gap calculation, within density-functional theory, we should have expected a rather poor description of a semimetallic behavior. Moreover, some theoretical investigations have already proved the general nonequivalence between experimental and Kohn-Sham Fermi surfaces.[36] Nevertheless, we have shown that a Kohn-Sham local-density approximation calculation of $A7$-structure semimetal Fermi surfaces gives correct location and shape of the Fermi surface, and provides a good estimation of the number of free carriers, albeit systematically too high. The comparison between theory and experiment is better than could have been expected from band-gap studies with the same formalism.

ACKNOWLEDGMENTS

One of the authors (X.G.) has benefited from the financial support of the National Fund for Scientific Research (Belgium). This paper presents research results of the Belgian Program on Interuniversity Attraction Poles initiated by the Belgian State—Prime Minister's Office—Science Policy Programming. We also acknowledge the use of the Namur Scientific Computing Facility (Namur-SCF), a common project between the FNRS, IBM Belgium, and the Facultés Universitaires Notre-Dame de la Paix (FUNDP).

APPENDIX

This Appendix summarizes the estimated uncertainties obtained on the band structure of As, Sb, and Bi. We will discuss more specifically the effects of the treatment of spin-orbit coupling, charge transfer, number of plane waves, and Brillouin-zone sampling discretization level. For the eight lower bands at the T, L, U, Γ, W, H, X, and K points, we have selected the maximum of the discrepancies between various approximations and the most accurate treatment. This value, representative of the whole band structure, has also been compared with the specific discrepancy for the overlap energy (which, by definition, is smaller).

The spin-orbit coupling affects each element differently. We also distinguish between the exact treatment, the restricted space treatment, and the complete neglect of spin-orbit contributions. Table IV gives the uncertainties, first for the general band structure, and secondly for the overlap energy. These two values widely differ. We observe that the restricted space treatment is adequate for As and Sb, but the exact treatment is preferable for Bi. We could include more than eight bands in the restricted space treatment. In this case the CPU time ratio with respect to the exact treatment changes, and becomes soon unfavorable (note that we use an iterative method[24]).

TABLE IV. Influence of the specific treatment of spin-orbit coupling on (a) the general band structure and (b) the overlap energy. All values are in meV.

	As	Sb	Bi
	(a)		
Exact treatment	0	0	0
Restricted set	11.7	68	425
Without s.o.	125	383	1420
	(b)		
Exact treatment	0	0	0
Restricted set	0.7	10.2	20
Without s.o.	6.2	40.5	518

The charge density can be constructed without any charge transfer. The small number of free carriers obtained experimentally gives an intuitive justification of this procedure. Moreover, the theoretical volume of the Fermi surface calculated with this charge density is comparable with the experimental one. To obtain an estimation of the accuracy of this procedure, we can construct a new charge density by adding to the semiconductor charge density the charge density of the experimental number of electrons at the L point and holes at H (for As and Sb) or T (for Bi) points. With this new density we compute the band structure and compare it to the band structure without charge transfer. The maximum discrepancies are 2 meV for As, 1 meV for Sb, and 0.01 meV for Bi. We believe that our treatment of the charge transfer should be valid for all semimetals. Its accuracy can be roughly estimated for $A7$-structure semimetals: approximately 2 meV for each 10^{-3} free electrons per atom. Further work is, of course, needed to determine the generality of such an estimation in other semimetals.

To generate an estimation of the number of special points needed, we have performed a study with a low number of plane waves: 10, 28, 60, and 110 special points in the irreducible part of the Brillouin zone, the last number being representative of perfect accuracy. The discrepancies for 10, 28, and 60 points are 30, 10, and 2 meV, respectively. From this result, the use of 60 points has been the general rule in this paper.

We have constructed the charge densities using wave functions described by 411 plane waves for Sb and Bi, and 405 for As, while for the precise eigenenergies computation, we used 605 plane waves for Sb and Bi, and 619 for As. The estimated discrepancies are 20 meV for a general point, and 2 meV for the overlap value.

All these values give a total truncation error on the overlap values of approximately 4 meV for Bi, 15 meV for Sb, and 7 meV for As.

[1]J. P. Issi, Aust. J. Phys. **32**, 585 (1979), and references therein.
[2]M. S. Dresselhaus, J. Phys. Chem. Solids **32**, 3 (1971), and references therein.
[3]S. Mase, J. Phys. Soc. Jpn. **13**, 434 (1958); **14**, 584 (1959).
[4]M. H. Cohen, L. M. Falicov, and S. Golin, IBM J. Res. Dev. **8**, 215 (1964).
[5]L. M. Falicov and S. Golin, Phys. Rev. **137**, A871 (1965).
[6]S. Golin, Phys. Rev. **140**, A993 (1965).
[7]P. J. Lin and L. M. Falicov, Phys. Rev. **142**, 441 (1966).
[8]S. Golin and J. A. Stocco, Phys. Rev. B **1**, 390 (1970).
[9]D. Weaire and A. R. Williams, in *The Physics of Semimetals and Narrow Gap Semiconductors,* edited by D. L. Carter and R. T. Bate (Pergamon, New York, 1971), p. 35; D. W. Bulett, Solid State Commun. **17**, 965 (1975); Y. Abe, I. Ohkoshi, and A. Morita, J. Phys. Soc. Jpn. **42**, 504 (1977); A. Morita, I. Ohkoshi, and Y. Abe, *ibid.* **43**, 1610 (1977); K. Shindo, *ibid.* **47**, 547 (1979); H. Tokailin, T. Takahashi, T. Sagawa, and K. Shindo, Phys. Rev. B **30**, 1765 (1984); T. Takahashi, H. Ohsawa, N. Gunasekara, H. Ishii, T. Kinoshita, T. Sagawa, H. Kato, T. Miyahara, and K. Shindo, Phys. Scr. **36**, 187 (1987).
[10]L. M. Falicov and P. J. Lin, Phys. Rev. **141**, 562 (1966); P. J. Lin and J. C. Phillips, *ibid.* **147**, 469 (1966).
[11]J. Rose and R. Schuchardt, Phys. Status Solidi B **117**, 213 (1983).
[12]S. Golin, Phys. Rev. **166**, 643 (1968); L. G. Ferreira, J. Phys. Chem. Solids **28**, 2891 (1967); **29**, 357 (1968); B. Norin, Phys. Scr. **15**, 341 (1977).
[13]R. J. Needs, R. M. Martin, and O. H. Nielsen, Phys. Rev. B **33**, 3778 (1986); **35**, 9851 (1987).
[14]K. J. Chang and M. L. Cohen, Phys. Rev. B **33**, 7371 (1986).
[15]L. F. Mattheis, D. R. Hamann, and W. Weber, Phys. Rev. B **34**, 2190 (1986).
[16]X. Gonze, J.-P. Michenaud, and J.-P. Vigneron, Phys. Scr. **37**, 785 (1988).
[17]From an atomic all-electron calculation. See Ref. 22 and D. Liberman, J. T. Waber, and D. T. Cromer, Phys. Rev. **137**, A27 (1965).
[18]D. Schiferl and C. S. Barrett, J. Appl. Crystallogr. **2**, 30 (1969).
[19]M. H. Cohen, Phys. Rev. **121**, 387 (1961).
[20]P. Hohenberg and W. Kohn, Phys. Rev. **136**, B864 (1964); W. Kohn and L. J. Sham, *ibid.* **140**, A1133 (1965).
[21]D. M. Ceperley and B. J. Alder, Phys. Rev. Lett. **45**, 566 (1980); J. Perdew and A. Zunger, Phys. Rev. B **23**, 5048 (1981).
[22]G. B. Bachelet, D. R. Hamann, and M. Schlüter, Phys. Rev. B **26**, 4199 (1982).
[23]J. Ihm, A. Zunger, and M. L. Cohen, J. Phys. C **12**, 4409 (1979).
[24]D. M. Wood and A. Zunger, J. Phys. A **18**, 1343 (1985).
[25]P. H. Dederichs and R. Zeller, Phys. Rev. B **28**, 5462 (1983).
[26]A. O. E. Animalu, Philos. Mag. **13**, 53 (1966).
[27]M. S. Hybertsen and S. G. Louie, Phys. Rev. B **34**, 2920 (1986).
[28]K. M. Rabe and J. D. Joannopoulos, Phys. Rev. B **32**, 2302 (1985); **36**, 3319 (1987).
[29]H. J. Monkhorst and J. D. Pack, Phys. Rev. B **13**, 5188 (1976).
[30]P. Lambin and J.-P. Vigneron, Phys. Rev. B **29**, 3430 (1984), and references therein.
[31]G. B. Bachelet, D. R. Hamann, and M. Schlüter, Phys. Rev. B **26**, 4206 (1979).
[32]See, for example, P. W. Atkins, *Molecular Quantum Mechanics,* 2nd ed. (Oxford University Press, Oxford, 1983), Chap. 10; G. B. Bachelet and N. E. Christensen, Phys. Rev. B **31**, 879 (1985).
[33]L. Ley, R. A. Pollak, S. P. Kowalczyk, R. McFeely, and D. A. Shirley, Phys. Rev. B **8**, 641 (1973).
[34]M. G. Priestley, L. R. Windmiller, J. B. Ketterson, and Y. Eckstein, Phys. Rev. **154**, 671 (1967).
[35]M. S. Hybertsen and S. G. Louie, Phys. Rev. Lett. **55**, 1418 (1985); Phys. Rev. B **34**, 5390 (1986); R. W. Godby, M. Schlüter, and L. J. Sham, Phys. Rev. Lett. **56**, 2415 (1986); Phys. Rev. B **35**, 4170 (1987); **36**, 3497 (1987); **37**, 10 159 (1988); J. E. Northrup, M. S. Hybertsen, and S. G. Louie, *ibid.* **39**, 8198 (1989). In the context of the semiconductor-semimetal transition, see R. W. Godby and R. J. Needs, Phys. Rev. Lett. **62**, 1169 (1989); X. Zhu, S. Fahy, and S. G. Louie, Phys. Rev. B **39**, 7840 (1989).
[36]D. Mearns, Phys. Rev. B **38**, 5906 (1988); K. Schönhammer and O. Gunnarsson, Phys. Rev. B **37**, 3128 (1988); N. H. March, *ibid.* **38**, 10 067 (1988).